THE JOURNAL OF BIOLOGICAL CHEMISTRY VOL. 288, NO. 30, pp. 21547–21557, July 26, 2013


# Hairy and Enhancer of Split-related with YRPW Motif (HEY)2 Regulates Bone Remodeling in Mice*

Received for publication, May 29, 2013 Published, JBC Papers in Press, June 19, 2013, DOI 10.1074/jbc.M113.489435

**Stefano Zanotti**[‡§] **and Ernesto Canalis**[‡§1]

*From the* [‡]*Department of Research, Saint Francis Hospital and Medical Center, Hartford, Connecticut 06105-1299 and the* [§]*University of Connecticut School of Medicine, Farmington, Connecticut 06030*

**Background:** Notch regulates bone mass and induces Hairy and Enhancer of Split-related with YRPW motif (HEY) in osteoblasts, but the skeletal function of individual HEY proteins is unclear.
**Results:** In male mice, *Hey2* inactivation increases bone mass, whereas HEY2 overexpression enhances bone resorption, reducing bone mass.
**Conclusion:** HEY2 regulates skeletal remodeling in male mice, decreasing bone mass.
**Significance:** HEY2 mediates selected skeletal effects of Notch.

**Notch induces Hairy and Enhancer of Split-related with YRPW motif *(Hey)1*, *Hey2*, and *HeyL* expression in osteoblasts, but the contributions of these genes to the skeletal effects of Notch are not fully understood. HEY1 misexpression has limited skeletal impact, female *HeyL* null mice display increased bone mass, and *Hey2* inactivation is developmentally lethal. To inactivate *Hey2* in immature or mature osteoblasts, $Hey2^{loxP/loxP}$ mice were crossed with transgenics expressing CRE under the control of the osterix (*Osx-Cre*) or osteocalcin (*Oc-Cre*) promoters to generate $Osx\text{-}Cre^{+/-}$;$Hey2^{\Delta/\Delta}$ or $Oc\text{-}Cre^{+/-}$;$Hey2^{\Delta/\Delta}$ mice. Trabecular bone volume increased in 3-month-old $Osx\text{-}Cre^{+/-}$;$Hey2^{\Delta/\Delta}$ and $Oc\text{-}Cre^{+/-}$;$Hey2^{\Delta/\Delta}$ male mice and in 1-month-old $Oc\text{-}Cre^{+/-}$;$Hey2^{\Delta/\Delta}$ female mice, although 3-month-old $Oc\text{-}Cre^{+/-}$;$Hey2^{\Delta/\Delta}$ females developed osteopenia. Alkaline phosphatase liver/bone/kidney (ALPL) expression and activity were suppressed in osteoblasts from $Oc\text{-}Cre^{+/-}$;$Hey2^{\Delta/\Delta}$ mice of both sexes. To overexpress HEY2 in osteoblasts, transgenic mice where a 3.6-kb fragment of the rat collagen type-I $\alpha$1 promoter directs HEY2 expression were created. Three-month-old *Hey2* transgenic males exhibited decreased osteoblast activity and increased bone resorption and developed osteopenia at 6 months of age. *Hey2* transgenic females exhibited reduced osteoblast number and function, but no changes in bone resorption. HEY2 overexpression in osteoblasts from mice of both sexes inhibited ALPL expression and activity and suppressed osteocalcin transcripts in cells from male mice only. HEY2 overexpression in osteoblasts from male mice enhanced bone resorption by co-cultured splenocytes and induced interleukin-6, a molecule that promotes osteoclastogenesis. In conclusion, HEY2 decreases skeletal mass and regulates bone remodeling in male mice.**

Hairy and Enhancer of Split (HES)[2]-related with YRPW motif (HEY) genes encode 3 helix-loop-helix transcription factors termed HEY1, HEY2, and HEY-Like (HEYL) (1–3). HEY proteins display structural similarities with HES transcription factors and are targets of canonical Notch signaling, a critical regulator of cell differentiation during development and postnatal life (4). HEY proteins play an important role in cardiovascular development. Inactivation of *Hey2* results in embryonic lethality due to cardiovascular defects, and the dual inactivation of *Hey1* and *Hey2* phenocopies the global deletion of *Notch1*. Similarly, the deletion of *Hey1* and *HeyL* impairs cardiovascular development in mice (5–9).

The continuous renewal of skeletal tissue is carried out in basic multicellular units. There, osteoclasts resorb bone, and following a reversal phase, new bone matrix is deposited by osteoblasts. Osteoblasts are derived from multipotent mesenchymal stem cells that can differentiate toward the osteoblastic, chondrocytic, or adipocytic lineages (10). The commitment of mesenchymal cells to the osteoblastic fate is controlled by a signaling network that includes bone morphogenetic proteins, Wnt, and Notch (11–16). Osteoclasts are multinucleated cells formed by fusion and osteoclastic differentiation of mononuclear cell precursors, a process that requires macrophage-colony stimulating factor (M-CSF) and the receptor activator of nuclear factor-$\kappa$b ligand (RANKL). RANK is expressed by osteoclast precursors and is activated following contact with cells expressing the membrane-bound RANKL. The activity of RANKL is opposed by osteoprotegerin (OPG), a soluble RANKL decoy receptor, and the ratio of RANKL over OPG regulates osteoclastogenesis (17, 18).

Notch is a transmembrane receptor activated by direct contact with Notch ligands. In the canonical signaling pathway, the Notch intracellular domain is released following a series of cleavages and forms a complex with Epstein-Barr virus latency

* This work was supported, in whole or in part, by National Institutes of Health Grant DK045227 from the NIDDK (to E. C.) and Research Fellowship Award 5371 from the Arthritis Foundation (to S. Z.).

[1] To whom correspondence should be addressed: Dept. of Research, Saint Francis Hospital and Medical Center, 114 Woodland St., Hartford, CT 06105-1299. Tel.: 860-714-4068; Fax: 860-714-8053; E-mail: ecanalis@stfranciscare.org.

[2] The abbreviations used are: HES, Hairy Enhancer of Split; HEY, HES-related with YRPW motif; HEYL, HEY-like; CTX-I, collagen type I C-terminal telopeptide; FVB, tropism to Friend leukemia virus strain-B; $\mu$CT, microcomputed tomography; OPG, osteoprotegerin; qRT-PCR, quantitative reverse transcription-PCR; RANKL, receptor activator of NF-$\kappa$-B ligand; Rpl38, ribosomal protein L38; SMI, structure model index.

C promoter binding factor 1, Suppressor of Hairless and Lag-1 (CSL), also termed Rbpjκ in mice, and with mastermind-like (MAML). The effects of Notch in the skeleton appear to be mediated by the canonical signaling pathway, but the genes responsible for the biology of Notch in bone have not been defined (19, 20). *Hes1*, *Hes5*, *Hey1*, *Hey2*, and *HeyL* are targets of the canonical Notch signaling pathway in skeletal cells, and as such should account, singly or in combination, for the effects of Notch in the skeleton (21). Previously, we reported that HES1 causes osteopenia by inhibiting bone formation and inducing bone resorption in mice (22). These effects of HES1 phenocopied only partially the skeletal phenotype of mice misexpressing Notch in the skeleton, suggesting that HEY proteins may be downstream effectors of Notch signaling in the skeleton (22). Transgenic expression of HEY1 under the control of the ubiquitously expressed β-actin promoter as well as the global inactivation of *Hey1* caused mild to modest osteopenia, and global *HeyL* null mice display increased bone mass (23, 24).

Notch signaling controls osteoclastic differentiation of bone marrow mononuclear precursors and the expression of RANKL and OPG in osteoblastic cells (15, 25, 26). Activation of the Notch signaling pathway in osteoclast precursors regulates osteoclastogenesis, and the cellular context or experimental conditions determine whether Notch suppresses or stimulates osteoclast differentiation (25–29).

In this study, we examined the function of HEY2 in the postnatal skeleton. For this purpose, the skeletal phenotype of mice misexpressing HEY2 was investigated by microcomputed tomography (μCT) and by histomorphometric analysis. To understand the cellular mechanisms involved, the differentiation and function of osteoblasts misexpressing HEY2 were examined *in vitro*.

## EXPERIMENTAL PROCEDURES

*Hey2 Conditional Null Mice*—To study the skeletal consequences of *Hey2* inactivation in cells of the osteoblastic lineage, mice where the *Hey2* sequence comprised between exon 1 and exon 4 was flanked by *loxP* sites in a 129Sv/C57BL/6 background, were provided by E. N. Olson (University of Texas Southwestern Medical Center, Dallas, TX) (6). To express CRE recombinase at early stages of osteoblastic differentiation, we obtained C57BL/6 mice where the CRE coding sequence is cloned downstream of an osterix (*Osx*) promoter (*Osx-Cre*) (The Jackson Laboratory) (30). In these mice, tetracycline suppresses the *Osx* promoter activity by virtue of a Tet-Off cassette (31). To express CRE preferentially in mature osteoblasts, mice where a 3.9-kb fragment of the human osteocalcin promoter directs CRE expression (*Oc-Cre*) were obtained from T. Clemens (Johns Hopkins Medicine, Baltimore, MD) and backcrossed for seven generations into a C57BL/6 genetic background. *Osx-Cre* or *Oc-Cre* transgenics were crossed with $Hey2^{loxP/loxP}$ mice to create $Osx\text{-}Cre^{+/-}$ or $Oc\text{-}Cre^{+/-}$;$Hey2^{loxP/wt}$ mice, which were mated with $Hey2^{loxP/loxP}$ to obtain $Osx\text{-}Cre^{+/-}$ or $Oc\text{-}Cre^{+/-}$;$Hey2^{loxP/loxP}$ mice. The latter were crossed with $Hey2^{loxP/loxP}$ to generate an experimental cohort, in which CRE excises the *loxP*-flanked sequences from the $Hey2^{loxP}$ allele ($Osx\text{-}Cre^{+/-}$ or $Oc\text{-}Cre^{+/-}$;$Hey2^{\Delta/\Delta}$) and littermate controls ($Hey2^{loxP/loxP}$). To prevent *Osx-Cre* expression during embryonic development, pregnant mothers were administered chow containing 625 mg/kg of doxycycline (Harlan Laboratories, Indianapolis, IN) from the time of conception to delivery. The presence of the *Osx-Cre* and *Oc-Cre* transgenes and of the $Hey2^{loxP}$ allele was determined by PCR in tail DNA extracts in newborns and adult mice, and primers specific for fatty acid-binding protein 1 (*Fabp1*) were used as positive controls in the PCR reactions. Recombination of sequences flanked by *loxP* sites was assessed by PCR in DNA extracts from parietal bone, using primers specific for the $Hey2^{\Delta}$ allele. All animal experiments were approved by the Animal Care and Use Committee of Saint Francis Hospital and Medical Center.

*Col3.6-Hey2 Transgenic Mice*—For preferential expression of HEY2 in osteoblasts, a 1047-bp DNA fragment coding for murine HEY2 (American Type Culture Collection; ATCC, Manassas, VA), preceded by a Kozak consensus sequence, was cloned downstream of a 3.6-kb fragment of the rat *Col1a1* (collagen type I α1) promoter and upstream of the bovine growth hormone polyadenylation signal (32). Microinjection of linearized DNA into pronuclei of fertilized oocytes from Friend leukemia virus strain B (FVB) mice (Charles River Laboratories, Wilmington, MA) and transfer of microinjected embryos into pseudopregnant mice were carried out at the Gene Targeting and Transgenic Facility of the University of Connecticut Health Center (Farmington, CT). Positive founders were identified by Southern blot analysis of tail DNA and bred to wild type FVB mice to create *Col3.6-Hey2* transgenic lines (33). To assess the effects of HEY2 overexpression, heterozygous *Col3.6-Hey2* mice were mated to wild type FVB mice to generate heterozygous *Col3.6-Hey2* transgenic mice and wild type littermate controls. The presence of the *Col3.6-Hey2* transgene was documented by PCR in tail DNA. To assess mRNA expression in skeletal cells, calvariae were frozen in liquid nitrogen at the time of harvest and transferred to −80 °C for storage before RNA extraction. To determine levels of bone resorption, fasting serum concentration of collagen type I C-terminal telopeptide (CTX-I), was measured by using the RatLaps enzyme-linked immunosorbent assay in accordance with the manufacturer's instructions (Immuno Diagnostic Systems, Scottsdale, AZ) (34).

*Microcomputed Tomography*—Femurs were scanned in 70% ethanol at an energy level of 55 kVp, an intensity of 145 μA, and an integration time of 200 ms on a μCT 40 scanner (Scanco Medical AG, Bassersdorf, Switzerland). Trabecular bone volume fraction and microarchitecture were evaluated starting ~1.0 mm proximal to the femoral condyles. A total of 160 consecutive slices acquired at an isotropic voxel size of 216 $\mu m^3$ and a slice thickness of 6 μm were chosen for analysis. Contours were manually drawn every 10 slices a few voxels away from the endocortical boundary to define the region of interest for analysis. The contours of the remaining slices were iterated automatically. Trabecular regions were assessed for bone volume fraction, trabecular thickness, number and separation, connectivity density, and structure model index (SMI), using a Gaussian filter ($\sigma = 0.8$) and a user-defined threshold (35). A total of 100 slices for the cortical region were measured at the mid-diaphysis of each femur with an isotropic voxel size of 216 $\mu m^3$ and a slice thickness of 6 μm. For mid-diaphysis analysis, con-

tours were iterated across the 100 slices along the cortical shell, excluding the bone marrow cavity. Analysis for cortical thickness was performed using a Gaussian filter ($\sigma = 0.8$) and a user-defined threshold (35).

*Bone Histomorphometric Analysis*—Static and dynamic histomorphometry of femurs was carried out after injection with 20 mg/kg calcein and 50 mg/kg demeclocycline, at an interval of 2 days for 1-month-old mice and 7 days for 3- and 6-month-old mice. Animals were sacrificed by $CO_2$ inhalation 2 days after the demeclocycline injection. Femurs were sectioned on a microtome at a thickness of 5 $\mu$m (Microm, Richards-Allan Scientific, Kalamazoo, MI) and stained with 0.1% toluidine blue. Static parameters of bone formation and resorption were measured in a defined area between 360 and 2160 $\mu$m from the growth plate, using an OsteoMeasure morphometry system (Osteometrics, Atlanta, GA) (36). For dynamic histomorphometry, mineralizing surface per bone surface and mineral apposition rate were measured on unstained sections under ultraviolet light, using a triple diamino-2-phenylindole fluorescein set long pass filter, and bone formation rate was calculated. The terminology and units used are those recommended by the Histomorphometry Nomenclature Committee of the American Society for Bone and Mineral Research (37).

*Osteoblast Cultures*—Osteoblast-enriched cells were isolated from parietal bones of 3–5-day-old male or female *Oc-Cre*$^{+/-}$;*Hey2*$^{\Delta/\Delta}$ or *Col3.6-Hey2* transgenic mice and littermate controls of the same sex by sequential collagenase digestion, as described (38). The sex of newborn mice was determined by PCR analysis of tail DNA with 5′-GAGAGCATGGAGGGCAT-3′ forward and 5′-GAGTACAGGTGTGCAGCTC-3′ reverse primers amplifying a 400-bp fragment of sex-determining region Y, located on chromosome Y, and with 5′-TGGACAGGACTGGACCTCTGCTTTCC-3′ forward and 5′-TAGAGCTTTGCCACATCACAGGTCAT-3′ reverse primers amplifying a 200-bp fragment of the autosomal gene fatty acid-binding protein 1. Cells were cultured in Dulbecco's modified Eagle's medium (DMEM, Life Technologies) supplemented with nonessential amino acids (Life Technologies), 20 mM HEPES, 100 $\mu$g/ml ascorbic acid (both from Sigma-Aldrich), and 10% fetal bovine serum (FBS; Atlanta Biologicals, Norcross, GA) at 37 °C in a humidified 5% $CO_2$ incubator.

*Quantitative Reverse Transcription-PCR (qRT-PCR)*—Total RNA was extracted from cells with the RNeasy mini kit, according to the manufacturer's instructions (Qiagen, Valencia, CA), and from frozen calvariae by phenol/chloroform extraction (Sigma-Aldrich), and changes in mRNA levels were determined by qRT-PCR. 0.5–1 $\mu$g of total RNA was reverse-transcribed using the iScript cDNA synthesis kit (Bio-Rad Laboratories) and amplified in the presence of 5′-TGGTATGGGCGTCTCCACAGTAACC-3′ forward and 5′-CTTGGAGAGGGCCACAAAGG-3′ reverse primers for alkaline phosphatase liver/bone/kidney (*Alpl*; NM_007431), 5′-CCCCTCTGGAAAGCTGTGGCGT-3′ forward and 5′-AGCTTCCCGTTCAGCTCTGG-3′ reverse primers for glyceraldehyde 3-phosphate dehydrogenase (*Gapdh*; NM_008084), 5′-AGCGAGAACAATTACCCTGGGCAC-3′ forward and 5′-ATTCTTGCCCTTCGCCTCTT-3′ reverse primers for *Hey2* (NM_013904), 5′-CGGCCTTCCCTACTTCACAAGTCCG-3′ forward and 5′-CAGGTCTGTTGGGAGTGGTATCC-3′ reverse primers for interleukin-6 (*Il6*; NM_031168), 5′-GACTCCGGCGCTACCTTGGGTAAG-3′ forward and 5′-CCCAGCACAACTCCTCCCTA-3′ reverse primers for osteocalcin (NM_001037939), 5′-CAGAAAGGAAATGCAACACATGACAAC-3′ forward and 5′-GCCTCTTCACACAGGGTGACATC-3′ reverse primers for osteoprotegerin (*Opg*; NM_008764), 5′-TATAGAATCCTGAGACTCCATGAAAAC-3′ forward and 5′-CCCTGAAAGGCTTGTTTCATCC-3′ reverse primers for *Rankl* (NM_011613), and 5′-AGAACAAGGATAATGTGAAGTTCAAGGTTC-3′ forward and 5′-CTGCTTCAGCTTCTCTGCCTTT-3′ reverse primers for ribosomal protein L38 (*Rpl38*; NM_001048057, NM_001048058, and NM_023372) and iQ SYBR Green supermix (Bio-Rad Laboratories) at 60 °C for 45 cycles, according to the manufacturer's instructions. Transcript copy number was estimated by comparison with a dilution series of *Alpl* and *Rpl38* (both from ATCC), *Gapdh* (R. Wu, Cornell University, Ithaca, NY), *Hey2* (T. Iso, University of Southern California, Los Angeles, CA), *Il6* and *Opg* (both from Open Biosystems, Huntsville, AL), osteocalcin (J. B. Lian, University of Massachusetts, Worcester, MA), and *Rankl* (Source BioScience, Nottingham, UK) cDNA (39–43). Reactions were conducted in a CFX96 qRT-PCR detection system (Bio-Rad Laboratories), and fluorescence was monitored at the annealing step of every PCR cycle. Specificity of the reaction was confirmed by the presence of a single peak in the melt curve analysis of PCR products.

*Alkaline Phosphatase Activity*—Alkaline phosphatase activity was determined in cell extracts by the hydrolysis of *p*-nitrophenyl phosphate to *p*-nitrophenol, measured by spectroscopy at 405 nm according to manufacturer's instructions (Sigma-Aldrich). Data are expressed as nanomoles of *p*-nitrophenol released per minute per $\mu$g of protein measured by the DC protein assay (Bio-Rad Laboratories).

*Osteoblast-Splenocyte Co-Cultures and Pit Formation Assay*—Primary osteoblasts from male *Col3.6-Hey2* transgenic mice and male littermate controls were seeded on BioCoat discs (BD Biosciences), and after reaching confluence, cultured in the presence of 100 $\mu$g/ml ascorbic acid and 5 mM $\beta$-glycerophosphate. Primary splenocytes were harvested from spleens aseptically removed from 1-month-old wild type FVB male mice, and $1 \times 10^6$ cells/cm$^2$ were seeded on the layer of primary osteoblasts in the presence of 10 nM 1,25 dihydroxyvitamin $D_3$ (BioMol International, Plymouth Meeting, PA) or phosphate-buffered saline, as control (44–46). Splenocytes and primary osteoblasts were cultured for 7 days, cells were removed with bleach for 5 min, and BioCoat discs were stained with von Kossa. Stained discs were photographed on a white light background and a digital grayscale image analyzed with Adobe Photoshop (Adobe Systems, Inc., San Jose, CA). The negative image was obtained with the invert feature of Adobe Photoshop, brightness and contrast were maximized, and the area of resorption was calculated as the percentage of pixels contained in half of the grayscale, determined by using the histogram function of Adobe Photoshop (22).

*Statistical Analysis*—Data are expressed as means ± S.E. Statistical differences were determined by Student's *t* test or anal-

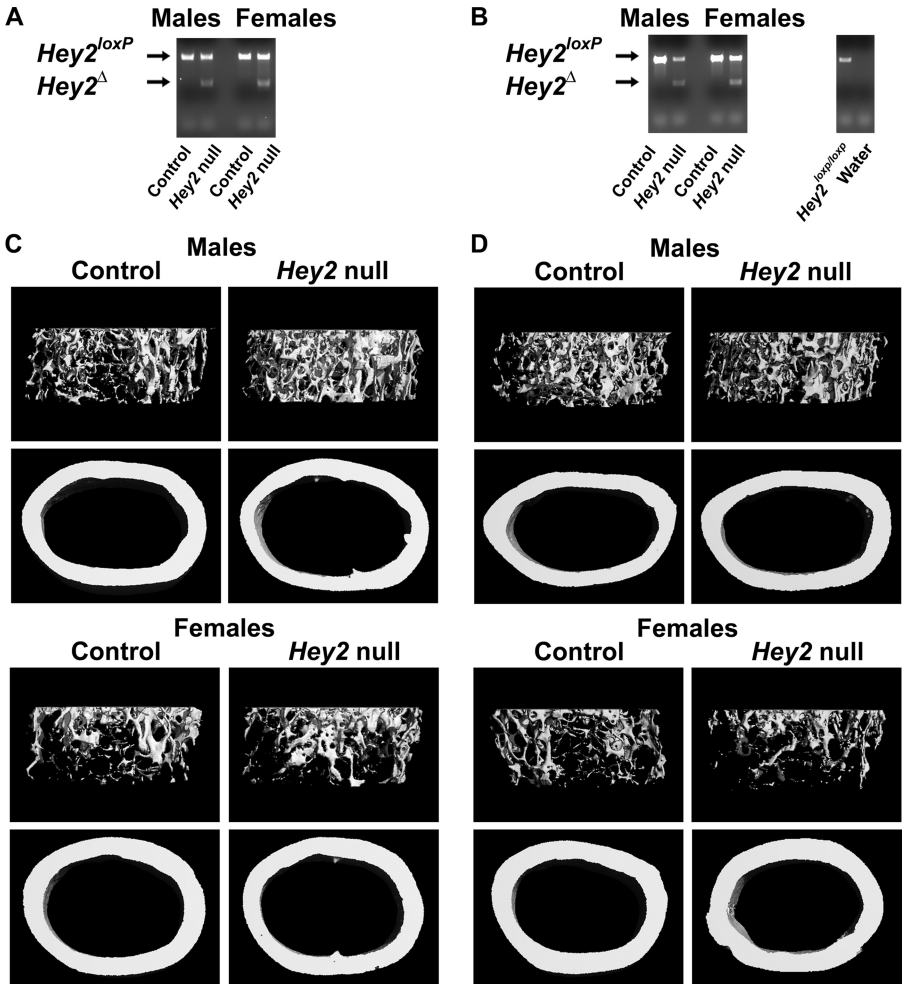


FIGURE 1. ***Hey2* inactivation in osteoblastic cells transiently increases trabecular bone volume in male mice.** In *A* and *B*, DNA was extracted from parietal bones of 3-month-old male or female *Osx-Cre*$^{+/-}$ (*A*) or *Oc-Cre*$^{+/-}$ (*B*); *Hey2*$^{\Delta/\Delta}$ mice (*Hey2* null), or littermate *Hey2*$^{loxP/loxP}$ controls of the same sex (*Control*). Recombination of the *Hey2*$^{loxP}$ allele was determined by PCR. Control reactions conducted in tail DNA from female *Hey2*$^{loxP/loxP}$ mouse or water were performed to confirm specificity of the primers. All reaction products were separated by electrophoresis on the same gel, and results from representative individuals are shown. *C* and *D* display microcomputed tomography images of proximal trabecular bone and cortical bone at the midshaft of femurs from representative 3-month-old male or female *Osx-Cre*$^{+/-}$ (*C*) or *Oc-Cre*$^{+/-}$ (*D*); *Hey2*$^{\Delta/\Delta}$ mice; (*Hey2* null) or littermate *Hey2*$^{loxP/loxP}$ controls of the same sex (*Control*).

ysis of variance with Schaeffe's post hoc analysis for pairwise or multiple comparisons, respectively (47).

## RESULTS

*Hey2 Inactivation in Cells of the Osteoblastic Lineage Causes a Transient Increase in Bone Volume*—To investigate the function of *Hey2* at early stages of osteoblast maturation and in differentiated osteoblasts, the skeletal phenotype of *Osx-Cre*$^{+/-}$;*Hey2*$^{\Delta/\Delta}$ or *Oc-Cre*$^{+/-}$;*Hey2*$^{\Delta/\Delta}$ mice was compared with the phenotype of littermate *Hey2*$^{loxP/loxP}$ controls of the same sex. Recombination of *Hey2* sequences flanked by *loxP* sites was detected in DNA extracts from calvariae of 1- and 3-month-old *Osx-Cre*$^{+/-}$;*Hey2*$^{\Delta/\Delta}$ and *Oc-Cre*$^{+/-}$;*Hey2*$^{\Delta/\Delta}$ mice, whereas recombination was not observed in littermate controls (Fig. 1, *A* and *B*, and data not shown). *Osx-Cre*$^{+/-}$;*Hey2*$^{\Delta/\Delta}$ and *Oc-Cre*$^{+/-}$;*Hey2*$^{\Delta/\Delta}$ mice were viable, appeared normal, and did not exhibit differences in mortality when compared with littermate controls.

In initial experiments, we demonstrated that *Oc-Cre*, *Osx-Cre*, and *Hey2*$^{loxP/loxP}$ did not exhibit an appreciable skeletal phenotype as determined by $\mu$CT at 1 month of age (48). One-month-old *Osx-Cre*$^{+/-}$;*Hey2*$^{\Delta/\Delta}$ male mice did not display a skeletal phenotype. $\mu$CT analysis of femurs from 3-month-old *Osx-Cre*$^{+/-}$;*Hey2*$^{\Delta/\Delta}$ male mice revealed increased trabecular bone volume and connectivity, secondary to increased trabecular number (Table 1, Fig. 1*C*). However, no changes in parameters of bone formation or bone resorption were observed by histomorphometric analysis (data not shown). No skeletal phenotype was observed in *Osx-Cre*$^{+/-}$;*Hey2*$^{\Delta/\Delta}$ female mice by $\mu$CT analysis (Table 1, Fig. 1*C*), indicating that *Hey2* inactivation at early stages of osteoblast differentiation increases bone mass only in male mice.

*Oc-Cre*$^{+/-}$;*Hey2*$^{\Delta/\Delta}$ male mice at 1 month of age did not exhibit changes in trabecular bone volume, although these mice displayed a limited reduction in mineral apposition rate and bone formation rate (Fig. 1*D*, Table 2). Three-month-old *Oc-Cre*$^{+/-}$;*Hey2*$^{\Delta/\Delta}$ male mice developed increased bone volume/tissue volume, indicating that the suppressed osteoblast function at 1 month of age does not translate into osteopenia in older mice (Table 2, Fig. 1*D*). In addition, inactivation of *Hey2* in 3-month-old male mice resulted in lower SMI (Table 2, Fig.

**TABLE 1**

**Microcomputed tomography (μCT) of the femur of 1- and 3-month-old *Osx-Cre*$^{+/-}$;*Hey2*$^{\Delta/\Delta}$ (*Hey2* null) male or female mice or littermate *Hey2*$^{loxP/loxP}$ controls (Control) of the same sex**

Values are means ± S.E.; $n = 5–9$. *, significantly different between *Hey2* null and control, $p < 0.05$; +, $p < 0.07$.

| | 1 month | | 3 month | |
|---|---|---|---|---|
| | Control | *Hey2* null | Control | *Hey2* null |
| **μCT (males)** | | | | |
| Bone volume fraction (%) | 4.9 ± 0.8 | 4.9 ± 0.6 | 4.1 ± 0.5 | 6.6 ± 0.8* |
| Trabecular separation (μm) | 243 ± 19 | 222 ± 7 | 236 ± 5 | 203 ± 5* |
| Trabecular number ($mm^{-1}$) | 4.3 ± 0.3 | 4.6 ± 0.1 | 4.2 ± 0.1 | 4.9 ± 0.1* |
| Trabecular thickness (μm) | 24.2 ± 1.0 | 23.4 ± 0.8 | 28.5 ± 0.5 | 30.0 ± 1.8 |
| Connectivity density ($mm^{-3}$) | 161 ± 38 | 192 ± 58 | 96 ± 18 | 218 ± 34* |
| Structure model index (SMI) | 2.97 ± 0.10 | 2.93 ± 0.10 | 2.98 ± 0.08 | 2.72 ± 0.09$^{+}$ |
| Cortical thickness (μm) | 102 ± 3 | 103 ± 2 | 165 ± 6 | 167 ± 6 |
| **μCT (females)** | | | | |
| Bone volume fraction (%) | 4.8 ± 0.6 | 4.0 ± 0.4 | 2.9 ± 0.4 | 3.3 ± 0.4 |
| Trabecular separation (μm) | 234 ± 16 | 244 ± 8 | 330 ± 12 | 294 ± 14 |
| Trabecular number ($mm^{-1}$) | 4.4 ± 0.3 | 4.2 ± 0.2 | 3.1 ± 0.1 | 3. 5 ± 0.1 |
| Trabecular thickness (μm) | 24.0 ± 0.6 | 22.7 ± 0.6 | 33.3 ± 0.5 | 32.4 ± 0.5 |
| Connectivity density ($mm^{-3}$) | 135 ± 25 | 110 ± 23 | 63 ± 11 | 92 ± 14 |
| Structure model index (SMI) | 2.85 ± 0.07 | 3.04 ± 0.07 | 3.04 ± 0.07 | 2.96 ± 0.10 |
| Cortical thickness (μm) | 100 ± 2 | 104 ± 1 | 178 ± 3 | 164 ± 5 |

**TABLE 2**

**Microcomputed tomography (μCT) and histomorphometry of the femur of 1, and 3 month old *Oc-Cre*$^{+/-}$;*Hey2*$^{\Delta/\Delta}$ (*Hey2* null) male or female mice, or littermate *Hey2*$^{loxP/loxP}$ (Control) of the same sex**

Values are means ± S.E.; $n = 4–9$. * Significantly between *Hey2* null and Control, $p < 0.05$; $+p < 0.07$.

| | 1 month | | 3 month | |
|---|---|---|---|---|
| | Control | *Hey2* null | Control | *Hey2* null |
| **μCT (males)** | | | | |
| Bone volume fraction (%) | 2.9 ± 0.6 | 2.8 ± 0.2 | 5.1 ± 0.6 | 6.9 ± 0.2* |
| Trabecular separation (μm) | 342 ± 27 | 321 ± 26 | 241 ± 12 | 221 ± 3 |
| Trabecular number ($mm^{-1}$) | 3.05 ± 0.28 | 3.22 ± 0.26 | 4.19 ± 0.18 | 4.49 ± 0.06 |
| Trabecular thickness (μm) | 22.3 ± 0.6 | 22.2 ± 0.6 | 30.9 ± 1.6 | 33.2 ± 0.8 |
| Connectivity density ($mm^{-3}$) | 103 ± 46 | 49 ± 12 | 127 ± 29 | 176 ± 10 |
| Structure model index (SMI) | 3.07 ± 0.15 | 3.16 ± 0.26 | 2.80 ± 0.07 | 2.60 ± 0.06* |
| Cortical thickness (μm) | 89 ± 2 | 87 ± 5 | 162 ± 1 | 170 ± 2* |
| **Histomorphometry (males)** | | | | |
| Bone volume/tissue volume (%) | 7.3 ± 1.0 | 4.8 ± 0.9 | 8.5 ± 1.2 | 9.9 ± 1.6 |
| Osteoblast surface/bone surface (%) | 23.2 ± 1.2 | 21.7 ± 1.8 | 12.8 ± 1.2 | 16.3 ± 1.0 |
| Osteoblasts/bone perimeter ($mm^{-1}$) | 20.4 ± 1.0 | 20.0 ± 1.1 | 14.2 ± 1.3 | 17.2 ± 1.9 |
| Osteoid surface/bone surface (%) | 3.9 ± 0.7 | 3.9 ± 0.5 | 1.1 ± .5 | 1.8 ± 0.5 |
| Osteoclast surface/bone surface (%) | 19.2 ± 1.3 | 19.3 ± 1.4 | 5.8 ± 0.7 | 5.2 ± 0.5 |
| Osteoclasts/bone perimeter ($mm^{-1}$) | 8.6 ± 0.7 | 9.1 ± 0.6 | 3.7 ± 0.6 | 3.4 ± 0.4 |
| Eroded surface/bone surface (%) | 20.4 ± 1.4 | 21.5 ± 1.0 | 9.4 ± 1.3 | 8.3 ± 0.7 |
| Mineral apposition rate ($\mu m\ day^{-1}$) | 1.22 ± 0.03 | 1.03 ± 0.03* | 1.65 ± 0.13 | 1.59 ± 0.03 |
| Mineralizing surface/bone surface (%) | 5.1 ± 1.2 | 2.4 ± 0.8 | 16.9 ± 4.3 | 19.1 ± 3.2 |
| Bone formation rate ($\mu m^2\ \mu m^{-3} day^{-1}$) | 0.06 ± 0.01 | 0.02 ± 0.01$^{+}$ | 0.29 ± 0.05 | 0.30 ± 0.05 |
| **μCT (females)** | | | | |
| Bone volume fraction (%) | 3.0 ± 0.4 | 3.5 ± 0.4 | 2.9 ± 0.3 | 1.9 ± 0.3* |
| Trabecular separation (μm) | 343 ± 28 | 293 ± 18 | 319 ± 10 | 360 ± 15* |
| Trabecular number ($mm^{-1}$) | 3.09 ± 0.23 | 3.52 ± 0.22 | 3.17 ± 0.09 | 2.82 ± 0.12* |
| Trabecular thickness (μm) | 23.3 ± 0.4 | 23.0 ± 0.4 | 33.6 ± 1.0 | 32.2 ± 1.7 |
| Connectivity density ($mm^{-3}$) | 64 ± 12 | 91 ± 24 | 57 ± 8 | 35 ± 8 |
| Structure model index (SMI) | 2.96 ± 0.04 | 2.91 ± 0.06 | 3.21 ± 0.10 | 3.36 ± 0.11 |
| Cortical thickness (μm) | 91 ± 1 | 92 ± 2 | 178 ± 3 | 173 ± 1 |
| **Histomorphometry (females)** | | | | |
| Bone volume/tissue volume (%) | 7.3 ± 0.6 | 5.8 ± 0.8 | 4.0 ± 0.4 | 3.4 ± 0.5 |
| Osteoblast surface/bone surface (%) | 21.8 ± 1.7 | 18.6 ± 2.2 | 27.0 ± 4.4 | 26.8 ± 4.9 |
| Osteoblasts/bone perimeter ($mm^{-1}$) | 19.1 ± 1.4 | 16.5 ± 1.5 | 28.3 ± 3.7 | 29.7 ± 4.2 |
| Osteoid surface/bone surface (%) | 4.2 ± 0.9 | 2.8 ± 0.6 | 4.8 ± 1.7 | 4.8 ± 1.8 |
| Osteoclast surface/bone surface (%) | 18.0 ± 0.4 | 19.3 ± 1.6 | 9.8 ± 1.1 | 10.2 ± 0.4 |
| Osteoclasts/bone perimeter ($mm^{-1}$) | 9.7 ± 0.2 | 10.3 ± 0.6 | 6.6 ± 0.7 | 6.9 ± 0.2 |
| Eroded surface/bone surface (%) | 23.7 ± 0.5 | 22.0 ± 1.2 | 14.9 ± 1.4 | 15.3 ± 0.5 |
| Mineral apposition rate ($\mu m\ day^{-1}$) | 1.32 ± 0.06 | 1.06 ± 0.08* | 2.46 ± 0.18 | 2.19 ± 0.40 |
| Mineralizing surface/bone surface (%) | 2.5 ± 0.4 | 2.6 ± 0.3 | 8.9 ± 1.6 | 6.7 ± 1.4 |
| Bone formation rate ($\mu m^2\ \mu m^{-3} day^{-1}$) | 0.03 ± 0.01 | 0.03 ± 0.01 | 0.22 ± 0.04 | 0.16 ± 0.05 |

1*D*), indicative of a higher ratio of plate-like over rod-like trabeculae (49). A modest increase in cortical thickness was observed (Table 2, Fig. 1*D*). Female *Oc-Cre*$^{+/-}$;*Hey2*$^{\Delta/\Delta}$ mice did not exhibit a skeletal phenotype at 1 month of age except for a modest reduction in mineral apposition rate, and at 3 months of age, they exhibited modest osteopenia by μCT, but not by histomorphometry (Table 2, Fig. 1*D*). The skeletal phenotypes of *Osx-Cre*$^{+/-}$;*Hey2*$^{\Delta/\Delta}$ and *Oc-Cre*$^{+/-}$;*Hey2*$^{\Delta/\Delta}$ mice were transient, and at 6 months of age, these mice were not different from littermate *Hey2*$^{loxP/loxP}$ controls, as determined by μCT (not shown).

*Hey2 Inactivation Impairs Osteoblast Function in Vitro*—To explore the cellular mechanisms that lead to suppressed bone

formation in *Oc-Cre*$^{+/-}$;*Hey2*$^{\Delta/\Delta}$ mice, primary osteoblastic cells were harvested from *Oc-Cre*$^{+/-}$;*Hey2*$^{\Delta/\Delta}$ male or female mice and littermate *Hey2*$^{loxP/loxP}$ controls of the same sex. Alkaline phosphatase transcripts and activity were decreased in the context of *Hey2* inactivation in primary calvarial osteoblasts from mice of both sexes (Fig. 2). These findings are in agreement with the decrease in mineral apposition rate exhibited by *Hey2* null mice and indicate that HEY2 is required for full osteoblastic function.

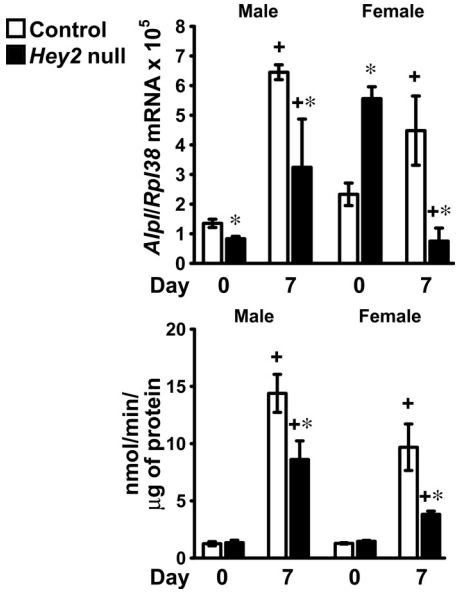


FIGURE 2. ***Hey2* inactivation inhibits osteoblast function *in vitro*.** Osteoblast-enriched cells were harvested from calvariae of male or female *Oc-Cre*$^{+/-}$;*Hey2*$^{\Delta/\Delta}$ mice (*Hey2 null*, *black bars*), or littermate *Hey2*$^{loxP/loxP}$ controls of the same sex (*Control*, *white bars*) and cultured under conditions favoring osteoblastogenesis. Total RNA was extracted, and mRNA was reverse-transcribed and amplified by qRT-PCR in the presence of specific primers. Data are expressed as *Alpl* copy number, corrected for *Rpl38* copy number. Values are means ± S.E., $n = 3–4$. Alkaline phosphatase activity was determined in cells extracted with Triton X-100, and data are expressed as nanomoles of *p*-nitrophenol/min/μg of total protein. Values are means ± S.E., $n = 6$. +, significantly different between day 7 and day 0, $p < 0.05$. *, significantly different between HEY2 and control, $p < 0.05$.

*HEY2 Overexpression in Osteoblasts Uncouples Bone Formation from Bone Resorption*—To test further the function of HEY2 in the skeleton, the effects of the preferential HEY2 overexpression in osteoblasts were investigated in *Col3.6-Hey2* transgenic mice at 1, 3, and 6 months of age. Three transgenic founders were obtained, and only one male founder mouse transmitted the transgene to the offspring, allowing the establishment of a *Hey2* transgenic line. *Col3.6-Hey2* transgenics were born at the expected Mendelian ratio and appeared normal and healthy. qRT-PCR analysis demonstrated that *Hey2* mRNA levels, corrected for *Rpl38* expression, in calvariae from 1-month-old *Col3.6-Hey2* transgenic males and females mice were increased 32.9 ± 3.4- and 32.2 ± 10.6-fold ($p < 0.05$), respectively, in comparison with control littermates of the same sex, confirming expression of the *Col3.6-Hey2* transgene.

μCT revealed that *Col3.6-Hey2* male transgenics did not exhibit a phenotype at 1 or 3 months of age, but were osteopenic at 6 months of age. The SMI value closer to 3 in the *Col3.6-Hey2* transgenic male mice indicated a preponderance of rod-like over plate-like trabeculae, suggesting that HEY2 affects bone microarchitecture (Table 3, Fig. 3) (49). Histomorphometric analysis revealed that *Col3.6-Hey2* transgenics had increased osteoclast number and eroded surface and decreased bone formation rate at 3 months of age (Table 3). However, HEY2 overexpression did not affect serum levels of CTX-I, a marker of bone resorption, in 1-month-old male mice (data not shown) (34). The changes in the cellular parameters observed at 3 months of age may explain the reduced bone volume observed in 6-month-old male mice, suggesting that overexpression of HEY2 in osteoblasts causes osteopenia due to an uncoupling of osteoblast and osteoclast activities.

μCT and histomorphometric analysis indicated that *Col3.6-Hey2* transgenic female mice did not exhibit an obvious skeletal phenotype at 1, 3, and 6 months of age, except for a decrease in bone formation rate at 6 months of age (Table 4, Fig. 3). No changes in osteoclast number, eroded surface, or serum levels of CTX-I were observed, indicating that HEY2 overexpression

**TABLE 3**

**Microcomputed tomography (μCT) and histomorphometry of the femur of 1, 3 and 6 month old *Col3.6-Hey2* transgenic male mice (HEY2), or littermate wild type controls of the same sex**

Values are means ± S.E.; $n = 5–10$. * Significantly between HEY2 and wild type, $p < 0.05$.

| | 1 month | | 3 month | | 6 month | |
|---|---|---|---|---|---|---|
| | Wild type | HEY2 | Wild type | HEY2 | Wild type | HEY2 |
| **μCT (males)** | | | | | | |
| Bone volume fraction (%) | 5.5 ± 0.8 | 7.5 ± 0.6 | 4.8 ± 0.5 | 4.7 ± 0.4 | 6.0 ± 0.8 | 3.2 ± 0.6* |
| Trabecular separation (μm) | 212 ± 11 | 204 ± 11 | 270 ± 10 | 259 ± 5 | 366 ± 3 | 356 ± 16 |
| Trabecular number ($mm^{-1}$) | 4.81 ± 0.24 | 5.03 ± 0.29 | 3.77 ± 0.13 | 3.91 ± 0.07 | 2.78 ± 0.01 | 2.84 ± 0.12 |
| Trabecular thickness (μm) | 24.7 ± 0.7 | 26.5 ± 0.3* | 29.8 ± 1.2 | 29.7 ± 0.9 | 38.2 ± 1.5 | 34.7 ± 2.1 |
| Connectivity density ($mm^{-3}$) | 213 ± 52 | 338 ± 44 | 138 ± 15 | 140 ± 14 | 103 ± 11 | 48 ± 10* |
| Structure model index (SMI) | 2.85 ± 0.11 | 2.52 ± 0.06* | 2.66 ± 0.13 | 2.75 ± 0.06 | 2.03 ± 0.15 | 2.74 ± 0.14* |
| Cortical thickness (μm) | 119 ± 2 | 117 ± 3 | 182 ± 4 | 177 ± 1 | 192 ± 3 | 189 ± 3 |
| **Histomorphometry (males)** | | | | | | |
| Bone volume/tissue volume (%) | 8.8 ± 0.4 | 9.9 ± 1.8 | 6.5 ± 0.6 | 7.6 ± 0.3 | 4.8 ± 0.9 | 3.5 ± 0.4 |
| Osteoblast surface/bone surface (%) | 17.0 ± 1.8 | 15.4 ± 2.2 | 12.7 ± 1.5 | 10.9 ± 1.1 | 11.1 ± 1.0 | 14.5 ± 1.4 |
| Osteoblasts/bone perimeter ($mm^{-1}$) | 17.2 ± 1.8 | 15.3 ± 2.4 | 15.5 ± 1.8 | 12.8 ± 1.4 | 11.4 ± 1.1 | 15.4 ± 2.4 |
| Osteoid surface/bone surface (%) | 1.0 ± 0.2 | 1.4 ± 0.3 | 0.9 ± 0.1 | 0.7 ± 0.2 | 0.8 ± 0.4 | 0.5 ± 0.2 |
| Osteoclast surface/bone surface (%) | 11.3 ± 0.7 | 10.4 ± 0.6 | 9.3 ± 0.5 | 10.9 ± 0.6 | 8.1 ± 0.4 | 8.3 ± 0.7 |
| Osteoclasts/bone perimeter ($mm^{-1}$) | 7.3 ± 0.4 | 7.1 ± 0.3 | 6.0 ± 0.3 | 7.2 ± 0.4* | 5.7 ± 0.3 | 5.8 ± 0.6 |
| Eroded surface/bone surface (%) | 23.1 ± 1.1 | 22.2 ± 1.5 | 13.8 ± 0.7 | 17.9 ± 1.0* | 13.8 ± 0.7 | 13.6 ± 1.1 |
| Mineral apposition rate ($\mu m\ day^{-1}$) | 2.53 ± 0.20 | 2.33 ± 0.17 | 0.60 ± 0.04 | 0.53 ± 0.03 | 0.49 ± 0.03 | 0.46 ± 0.04 |
| Mineralizing surface/bone surface (%) | 3.0 ± 0.3 | 3.3 ± 0.5 | 10.9 ± 1.0 | 6.5 ± 1.0* | 5.5 ± 1.2 | 8.2 ± 2.0 |
| Bone formation rate ($\mu m^2\ \mu m^{-3} day^{-1}$) | 0.08 ± 0.01 | 0.08 ± 0.02 | 0.07 ± 0.01 | 0.04 ± 0.01* | 0.03 ± 0.01 | 0.04 ± 0.01 |

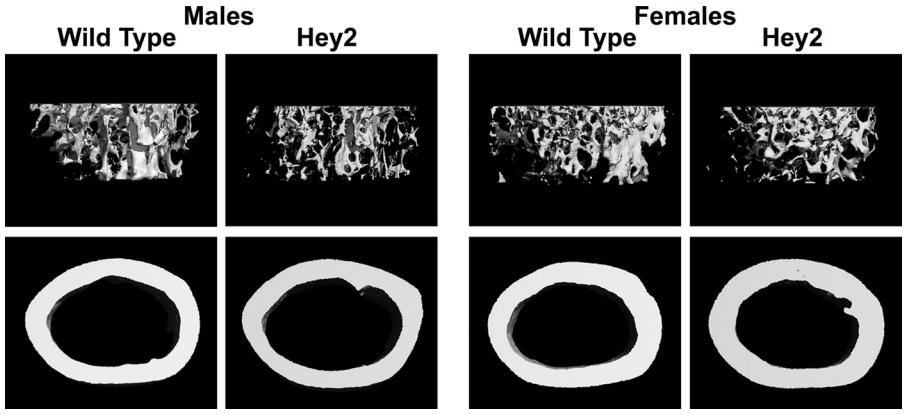


FIGURE 3. ***Hey2* overexpression in osteoblasts causes osteopenia in male mice.** Microcomputed tomography images of proximal trabecular bone and cortical bone at the midshaft of femurs from representative 6-month-old male or female *Col3.6-Hey2* transgenic mice (*Hey2*) or littermate wild type controls of the same sex (*Wild Type*) are shown.

**TABLE 4**

**Microcomputed tomography ($\mu$CT) and histomorphometry of the femur of 1, 3 and 6 month old *Col3.6-Hey2* transgenic female mice (HEY2) or littermate wild type controls of the same sex**

Values are means ± S.E.; $n = 4-8$. * Significantly between HEY2 and wild type, $p < 0.05$. + $p < 0.51$.

| | 1 month | | 3 month | | 6 month | |
|---|---|---|---|---|---|---|
| | Wild type | HEY2 | Wild type | HEY2 | Wild type | HEY2 |
| **$\mu$CT (females)** | | | | | | |
| Bone volume fraction (%) | 7.0 ± 0.6 | 7.2 ± 0.8 | 4.6 ± 0.2 | 4.8 ± 0.4 | 4.7 ± 1.4 | 5.1 ± 0.6 |
| Trabecular separation ($\mu$m) | 192 ± 9 | 193 ± 11 | 281 ± 4 | 291 ± 10 | 337 ± 25 | 324 ± 11 |
| Trabecular number ($mm^{-1}$) | 5.28 ± 0.25 | 5.25 ± 0.31 | 3.63 ± 0.45 | 3.52 ± 0.11 | 3.11 ± 0.26 | 3.17 ± 0.11 |
| Trabecular thickness ($\mu$m) | 26.7 ± 0.6 | 26.4 ± 0.8 | 32.8 ± 0.4 | 34.6 ± 0.7 | 35.8 ± 0.9 | 37.0 ± 0.9 |
| Connectivity density ($mm^{-3}$) | 264 ± 34 | 293 ± 46 | 109 ± 7 | 113 ± 15 | 98 ± 43 | 101 ± 15 |
| Structure model index (SMI) | 2.66 ± 0.06 | 2.66 ± 0.09 | 2.88 ± 0.02 | 2.69 ± 0.09 | 2.72 ± 0.23 | 2.36 ± 0.06 |
| Cortical thickness ($\mu$m) | 124 ± 2 | 122 ± 3 | 177 ± 2 | 182 ± 2 | 201 ± 3 | 208 ± 2* |
| **Histomorphometry (females)** | | | | | | |
| Bone volume/tissue volume (%) | 10.2 ± 0.8 | 11.5 ± 0.7 | 6.1 ± 0.7 | 5.5 ± 0.5 | 4.4 ± 0.7 | 5.7 ± 0.9 |
| Osteoblast surface/bone surface (%) | 20.7 ± 2.6 | 17.8 ± 1.3 | 18.0 ± 1.3 | 15.0 ± 0.7+ | 16.6 ± 1.0 | 20.0 ± 2.2 |
| Osteoblasts/bone perimeter ($mm^{-1}$) | 20.7 ± 2.3 | 17.3 ± 1.3 | 21.5 ± 1.4 | 17.7 ± 0.6* | 17.5 ± 0.8 | 19.1 ± 1.9 |
| Osteoid surface/bone surface (%) | 2.8 ± 0.5 | 1.3 ± 0.2* | 2.8 ± 0.6 | 1.7 ± 0.3 | 1.5 ± 0.3 | 1.5 ± 0.6 |
| Osteoclast surface/bone surface (%) | 10.2 ± 0.3 | 10.4 ± 0.8 | 12.7 ± 0.7 | 13.0 ± 0.4 | 11.5 ± 1.0 | 11.3 ± 0.9 |
| Osteoclasts/bone perimeter ($mm^{-1}$) | 7.1 ± 0.2 | 7.5 ± 0.6 | 8.8 ± 0.5 | 9.1 ± 0.3 | 8.0 ± 0.6 | 7.9 ± 0.6 |
| Eroded surface/bone surface (%) | 21.8 ± 1.4 | 23.4 ± 1.5 | 22.1 ± 1.2 | 22.7 ± 1.0 | 20.3 ± 1.4 | 19.6 ± 1.1 |
| Mineral apposition rate ($\mu m\ day^{-1}$) | 2.80 ± 0.22 | 2.73 ± 0.14 | 0.90 ± 0.03 | 0.76 ± 0.03* | 0.75 ± 0.05 | 0.58 ± 0.04* |
| Mineralizing surface/bone surface (%) | 4.5 ± 0.5 | 5.5 ± 0.7 | 12.2 ± 2.5 | 10.5 ± 0.9 | 16.2 ± 1.3 | 12.8 ± 2.0 |
| Bone formation rate ($\mu m^2\ \mu m^{-3} day^{-1}$) | 0.12 ± 0.02 | 0.16 ± 0.03 | 0.11 ± 0.02 | 0.08 ± 0.01 | 0.12 ± 0.01 | 0.08 ± 0.01* |

in osteoblasts regulates osteoclast differentiation and function only in male mice.

*HEY2 Overexpression Impairs Osteoblast Function in Vitro*—To understand the cellular effects caused by HEY2 overexpression, osteoblast-enriched cells were harvested from calvariae of *Hey2* transgenic male or female mice and littermate controls of the same sex. Increased HEY2 transcripts were confirmed by qRT-PCR in osteoblasts from *Col3.6-Hey2* transgenics over a 14-day culture period (Fig. 4). Alkaline phosphatase transcripts and activity were suppressed by HEY2 in cells from both sexes (Fig. 4). Osteocalcin expression was detected only at 7 and 14 days of culture and was suppressed in osteoblasts from *Col3.6-Hey2* male but not female transgenic mice (Fig. 4). These findings confirm that HEY2 overexpression impairs osteoblast differentiation and function in both sexes and could explain the decreased bone formation and osteoblast number observed *in vivo*.

*HEY2 Overexpression Enhances Osteoclast Function in Vitro*—To determine whether the overexpression of HEY2 regulated osteoclast differentiation or function, calvariae from male *Col3.6-Hey2* transgenics and littermate wild type controls were co-cultured with wild type FVB splenocytes, a source of mononuclear osteoclast precursors. Treatment with 1,25-dihydroxyvitamin $D_3$ induced resorptive activity of wild type splenocytes, and in agreement with the increased eroded surface and osteoclast number observed in the *Col3.6-Hey2* transgenic males, osteoblasts from *Col3.6-Hey2* transgenics enhanced resorption (Fig. 5*A*) (44). To investigate possible mechanisms for the stimulatory effect of HEY2 on bone resorption, interleukin-6 (IL6) *Rankl* and *Opg* mRNA levels were determined (50). An increase in IL6 transcripts was observed only in male *Col3.6-Hey2* transgenic osteoblasts (Fig. 5*B*), suggesting that HEY2 increases bone resorption by inducing the expression of IL6. HEY2 caused a modest and unexplained increase in *Rankl* transcripts in osteoblasts from female mice. In accordance with the effects of Notch on OPG expression, HEY2 induced *Opg* mRNA levels in cells from male mice (Fig. 5*B*) (26, 48). This may represent an indirect compensatory mechanism to temper the effects of HEY2 on osteoclastogenesis.

## DISCUSSION

In this study, we investigated the skeletal function of *Hey2*, a Notch target gene. *Hey2* inactivation in cells of the osteoblastic lineage caused an increase in trabecular bone volume, an effect

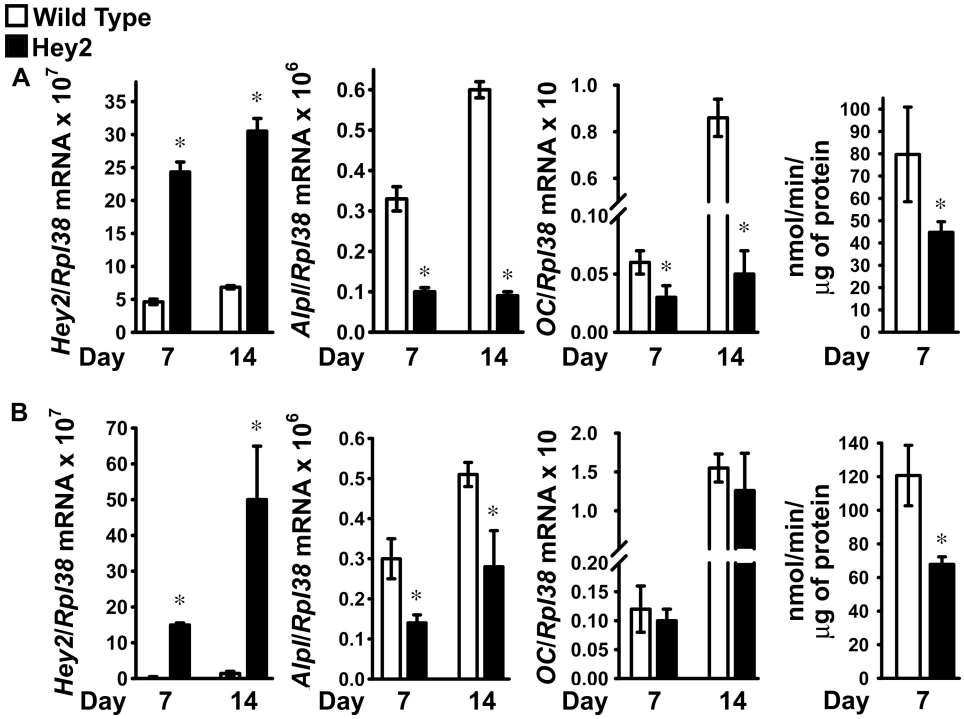


FIGURE 4. **HEY2 overexpression suppresses osteoblast function *in vitro*.** *A* and *B*, osteoblast-enriched cells were harvested from the calvariae of male (*A*) or female (*B*) *Col3.6-Hey2* transgenic mice (*Hey2*, *black bars*) or littermate wild type controls of the same sex (*Wild Type*, *white bars*) and cultured under conditions favoring osteoblastogenesis. Total RNA was extracted, and mRNA was reverse-transcribed and amplified by qRT-PCR in the presence of specific primers. Data are expressed as *Hey2*, *Alpl*, and osteocalcin (*OC*) copy number, corrected for *Rpl38* copy number. Values are means ± S.E., $n = 4$. Alkaline phosphatase activity was determined in cells extracted with Triton X-100, and data are expressed as nanomoles of *p*-nitrophenol/min/$\mu$g of total protein. Values are means ± S.E., $n = 6$. *, significantly different between HEY2 and wild type, $p < 0.05$.

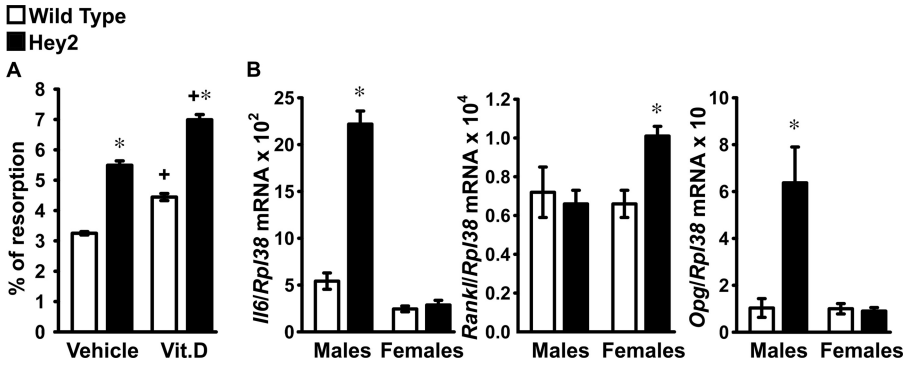


FIGURE 5. **HEY2 overexpression in osteoblasts from male mice induces resorption by co-cultured splenocytes and IL6 expression *in vitro*.** Osteoblast-enriched cells were harvested from calvariae of male or female *Col3.6-Hey2* transgenics (*Hey2*, *black bars*), or littermate wild type controls of the same sex (*Wild Type*, *white bars*) and cultured under conditions favoring osteoblastogenesis. In *A*, osteoblast-enriched cells from male mice were co-cultured with splenocytes from wild type mice of the same sex in the presence of 10 nM 1,25-dihydroxyvitamin $D_3$ (*Vit.D*) or vehicle. After 7 days, cells were removed with bleach, the culture substrate was stained by Von Kossa, and digital pictures were acquired for the estimation of the resorbed area. Data are expressed as the percentage of the resorbed area. Values are means ± S.E., $n = 4–6$. *, significantly different between HEY2 and wild type, $p < 0.05$. +, significantly different between 1,25-dihydroxyvitamin $D_3$ and vehicle, $p < 0.05$. In *B*, total RNA was extracted from osteoblast-enriched cell cultures at confluence, and mRNA was reverse-transcribed and amplified by qRT-PCR in the presence of specific primers. Data are expressed as *Il6*, *Rankl*, and *Opg* copy number, corrected for *Gapdh* copy number. Values are means ± S.E., $n = 4$. *, significantly different between HEY2 and wild type, $p < 0.05$.

that is consistent with the osteopenic phenotype caused by the activation of Notch signaling in these cells (16, 48). The skeletal phenotype was mild, transient, and more pronounced in male than in female mice, indicating that *Hey2* plays a modest role in skeletal homeostasis. Inactivation of *Hey2* at early stages of osteoblastic differentiation did not affect the number or function of skeletal cells, and a developmental nature for the increased bone mass is excluded because the activity of the *Osx* promoter was suppressed by doxycycline during embryonic development (30). Global *HeyL* null mice carrying a heterozygous null mutation of *Hey1* exhibit increased bone mass, indicating that *Hey1*, *HeyL*, and *Hey2* have similar functions in the skeleton (24). It is plausible that *Hey1* and *HeyL* compensate for the loss of *Hey2* function, preventing detection of subtle changes in osteoblast and osteoclast number and activity, which lead to a modest increase in bone mass. Compensation by *Hey1* might explain the sexually dimorphic skeletal phenotype of *Hey2* inactivation in immature osteoblastic cells because *Hey1* transcript levels significantly increased 1.4-fold in parietal bones when *Hey2* was inactivated in female mice, but not in

male mice (data not shown). Inactivation of *Hey2* in osteoblasts did not affect serum markers of bone remodeling and transiently inhibited bone formation, but the effect was modest, confirming that *Hey2* has a limited impact on skeletal function.

Although three *Hey2* transgenic founders were obtained, only one transgenic line was established, indicating that excessive levels of HEY2 in cells expressing the 3.6-kb fragment of the *Col1a1* promoter are detrimental for embryonic development. The activity of this promoter fragment is not restricted to osteoblastic cells, and expression of HEY2 in nonskeletal tissues may have prevented transmission of the transgene (51, 52). Despite these limitations, the data indicate that HEY2 overexpression affects bone remodeling and uncouples bone formation from bone resorption by increasing osteoclastogenesis in male mice and by suppressing osteoblast number and function in both genders. In accordance with the effects of the *Hey2* inactivation in osteoblastic cells, *Col3.6-Hey2* transgenic male mice displayed osteopenia and impaired trabecular microarchitecture at 6 months of age. However, the inhibition of osteoblast number and activity in female mice did not result in changes in trabecular volume or structure. There is no immediate explanation for the discrepancy in the skeletal phenotype of male and female transgenics, and it is conceivable that mechanisms necessary for the protection of bone mass are at play in female mice in the context of HEY2 overexpression. Alternatively, a variable penetrance of the *Col3.6-Hey2* transgene may be responsible for the absence of changes in trabecular bone of female transgenics.

The differences between the skeletal phenotypes observed in the two sexes also could be explained by a sexually dimorphic mechanism of HEY2 action in osteoblasts. HEY2 is a paralogue of HES1, and HES1 overexpression under the control of the 3.6-kb fragment of the *Col1a1* promoter induces osteoclastogenesis in male mice and suppresses osteoblastogenesis in female mice, confirming that the skeletal effects of the HES and HEY families of proteins are sexually dimorphic (22). An explanation for the sexual dimorphism could be provided by the protective effects of estrogens on skeletal mass (53).

*In vitro* studies exploring the differentiation and function of osteoblastic cells from mice misexpressing *Hey2* indicate that HEY2 is dispensable for osteoblastogenesis and that perturbation of its expression in mature cells suppresses osteoblast function in both male and female mice. Although the mechanism was not established, it is possible that HEY2, like HEY1, interacts with transcription factors necessary for osteoblastogenesis, such as Runx2 (15). The decreased osteoblastic function by *Hey2* inactivation is not consistent with the effects of Notch on mature cells of the osteoblastic lineage. The suppressive effects of HEY2 on transcription might explain this discrepancy because the absence of HEY2 might lead to increased expression of inhibitors of osteoblastic function (1, 3). Results from cells overexpressing HEY2 are in agreement with the inhibitory effects of Notch overexpression on osteoblast function (4). Overexpression of HEY2 in osteoblasts causes a less severe skeletal phenotype than the one observed following the induction of Notch under the control of the 3.6-kb fragment of the *Col1a1* promoter. This may suggest that the skeletal effects of Notch require expression of additional targets of Notch signaling, such as HES1, or are primarily mediated by direct regulation of osteoblast-specific genes by Notch (16).

The increased bone resorption reported in *Hey2* transgenic mice does not phenocopy the inhibitory effect of Notch on osteoclastogenesis, which is mediated by an induction of OPG and suppression of RANKL and M-CSF expression by osteoblastic cells (15, 25, 26, 48). HES1 is an inducer of osteoclastogenesis, suggesting that HEY and HES transcription factors carry out functions that are independent from their role as targets of Notch signaling (22). We report an induction of *Il6* expression by HEY2 in osteoblasts from male mice, suggesting a possible mechanism for the enhanced bone resorption observed in male *Col3.6-Hey2* transgenics. However, HEY2, like Notch, induced OPG expression, and this may be a protective mechanism to prevent excessive osteoclastogenesis. IL6 serum levels were not increased in *Col3.6-Hey2* transgenic mice (data not shown), indicating that IL6 acts locally to regulate bone resorption. Although IL6 regulates osteoclastogenesis by inducing RANKL in osteoblastic cells, its direct effects on cells of the osteoclast lineage are less clear, and both a stimulatory function and an inhibitory function of IL6 in the differentiation of osteoclast precursors have been reported (54, 55). Our observations indicate that in the context of HEY2 overexpression, IL6 promotes the resorptive activity of osteoclast precursors.

In conclusion, *Hey2* plays a modest role in the regulation of skeletal cell function, whereas HEY2 overexpression in male mice uncouples bone formation from bone resorption, causes osteopenia, and compromises bone microarchitecture.

*Acknowledgments—We thank Drs. E. Olson for Hey2$^{loxP/loxP}$ conditional mice, T. Clemens for osteocalcin-CRE transgenics, J. B. Lian for osteocalcin, and R. Wu for GAPDH cDNA. We thank A. Kent, K. Parker, and L. Kranz for technical support and M. Yurczak for secretarial assistance.*

## REFERENCES

1. Iso, T., Kedes, L., and Hamamori, Y. (2003) HES and HERP families: multiple effectors of the Notch signaling pathway. *J. Cell Physiol.* **194,** 237–255
2. Kageyama, R., Ohtsuka, T., and Kobayashi, T. (2007) The Hes gene family: repressors and oscillators that orchestrate embryogenesis. *Development* **134,** 1243–1251
3. Fischer, A., and Gessler, M. (2007) Delta–Notch—and then? Protein interactions and proposed modes of repression by Hes and Hey bHLH factors. *Nucleic Acids Res.* **35,** 4583–4596
4. Zanotti, S., and Canalis, E. (2010) Notch and the skeleton. *Mol. Cell Biol.* **30,** 886–896
5. Kokubo, H., Miyagawa-Tomita, S., Tomimatsu, H., Nakashima, Y., Nakazawa, M., Saga, Y., and Johnson, R. L. (2004) Targeted disruption of *hesr2* results in atrioventricular valve anomalies that lead to heart dysfunction. *Circ. Res.* **95,** 540–547
6. Xin, M., Small, E. M., van Rooij, E., Qi, X., Richardson, J. A., Srivastava, D., Nakagawa, O., and Olson, E. N. (2007) Essential roles of the bHLH transcription factor Hrt2 in repression of atrial gene expression and maintenance of postnatal cardiac function. *Proc. Natl. Acad. Sci. U.S.A.* **104,** 7975–7980
7. Fischer, A., Steidl, C., Wagner, T. U., Lang, E., Jakob, P. M., Friedl, P., Knobeloch, K. P., and Gessler, M. (2007) Combined loss of *Hey1* and *HeyL* causes congenital heart defects because of impaired epithelial to mesenchymal transition. *Circ. Res.* **100,** 856–863

8. Fischer, A., Schumacher, N., Maier, M., Sendtner, M., and Gessler, M. (2004) The Notch target genes *Hey1* and *Hey2* are required for embryonic vascular development. *Genes Dev.* **18,** 901–911
9. Kokubo, H., Miyagawa-Tomita, S., Nakazawa, M., Saga, Y., and Johnson, R. L. (2005) Mouse *hesr1* and *hesr2* genes are redundantly required to mediate Notch signaling in the developing cardiovascular system. *Dev. Biol.* **278,** 301–309
10. Bianco, P., and Gehron Robey, P. (2000) Marrow stromal stem cells. *J. Clin. Invest.* **105,** 1663–1668
11. Canalis, E., Giustina, A., and Bilezikian, J. P. (2007) Mechanisms of anabolic therapies for osteoporosis. *N. Engl. J. Med.* **357,** 905–916
12. Canalis, E., Economides, A. N., and Gazzerro, E. (2003) Bone morphogenetic proteins, their antagonists, and the skeleton. *Endocr. Rev.* **24,** 218–235
13. Westendorf, J. J., Kahler, R. A., and Schroeder, T. M. (2004) Wnt signaling in osteoblasts and bone diseases. *Gene* **341,** 19–39
14. Engin, F., Yao, Z., Yang, T., Zhou, G., Bertin, T., Jiang, M. M., Chen, Y., Wang, L., Zheng, H., Sutton, R. E., Boyce, B. F., and Lee, B. (2008) Dimorphic effects of Notch signaling in bone homeostasis. *Nat. Med.* **14,** 299–305
15. Hilton, M. J., Tu, X., Wu, X., Bai, S., Zhao, H., Kobayashi, T., Kronenberg, H. M., Teitelbaum, S. L., Ross, F. P., Kopan, R., and Long, F. (2008) Notch signaling maintains bone marrow mesenchymal progenitors by suppressing osteoblast differentiation. *Nat. Med.* **14,** 306–314
16. Zanotti, S., Smerdel-Ramoya, A., Stadmeyer, L., Durant, D., Radtke, F., and Canalis, E. (2008) Notch inhibits osteoblast differentiation and causes osteopenia. *Endocrinology* **149,** 3890–3899
17. Lacey, D. L., Timms, E., Tan, H. L., Kelley, M. J., Dunstan, C. R., Burgess, T., Elliott, R., Colombero, A., Elliott, G., Scully, S., Hsu, H., Sullivan, J., Hawkins, N., Davy, E., Capparelli, C., Eli, A., Qian, Y. X., Kaufman, S., Sarosi, I., Shalhoub, V., Senaldi, G., Guo, J., Delaney, J., and Boyle, W. J. (1998) Osteoprotegerin ligand is a cytokine that regulates osteoclast differentiation and activation. *Cell* **93,** 165–176
18. Teitelbaum, S. L. (2007) Osteoclasts: what do they do and how do they do it? *Am. J. Pathol.* **170,** 427–435
19. Dong, Y., Jesse, A. M., Kohn, A., Gunnell, L. M., Honjo, T., Zuscik, M. J., O'Keefe, R. J., and Hilton, M. J. (2010) RBPj$\kappa$-dependent Notch signaling regulates mesenchymal progenitor cell proliferation and differentiation during skeletal development. *Development* **137,** 1461–1471
20. Tao, J., Chen, S., Yang, T., Dawson, B., Munivez, E., Bertin, T., and Lee, B. (2010) Osteosclerosis owing to Notch gain of function is solely Rbpj-dependent. *J. Bone Miner Res.* **25,** 2175–2183
21. Zanotti, S., Smerdel-Ramoya, A., and Canalis, E. (2011) Reciprocal regulation of Notch and nuclear factor of activated T-cells (NFAT) c1 transactivation in osteoblasts. *J. Biol. Chem.* **286,** 4576–4588
22. Zanotti, S., Smerdel-Ramoya, A., and Canalis, E. (2011) HES1 (hairy and enhancer of split 1) is a determinant of bone mass. *J. Biol. Chem.* **286,** 2648–2657
23. Salie, R., Kneissel, M., Vukevic, M., Zamurovic, N., Kramer, I., Evans, G., Gerwin, N., Mueller, M., Kinzel, B., and Susa, M. (2010) Ubiquitous overexpression of Hey1 transcription factor leads to osteopenia and chondrocyte hypertrophy in bone. *Bone* **46,** 680–694
24. Tu, X., Chen, J., Lim, J., Karner, C. M., Lee, S. Y., Heisig, J., Wiese, C., Surendran, K., Kopan, R., Gessler, M., and Long, F. (2012) Physiological notch signaling maintains bone homeostasis via RBPjk and Hey upstream of NFATc1. *PLoS. Genet.* **8,** e1002577
25. Yamada, T., Yamazaki, H., Yamane, T., Yoshino, M., Okuyama, H., Tsuneto, M., Kurino, T., Hayashi, S., and Sakano, S. (2003) Regulation of osteoclast development by Notch signaling directed to osteoclast precursors and through stromal cells. *Blood* **101,** 2227–2234
26. Bai, S., Kopan, R., Zou, W., Hilton, M. J., Ong, C. T., Long, F., Ross, F. P., and Teitelbaum, S. L. (2008) NOTCH1 regulates osteoclastogenesis directly in osteoclast precursors and indirectly via osteoblast lineage cells. *J. Biol. Chem.* **283,** 6509–6518
27. Fukushima, H., Nakao, A., Okamoto, F., Shin, M., Kajiya, H., Sakano, S., Bigas, A., Jimi, E., and Okabe, K. (2008) The association of Notch2 and NF-$\kappa$B accelerates RANKL-induced osteoclastogenesis. *Mol. Cell Biol.* **28,** 6402–6412
28. Sethi, N., Dai, X., Winter, C. G., and Kang, Y. (2011) Tumor-derived JAGGED1 promotes osteolytic bone metastasis of breast cancer by engaging notch signaling in bone cells. *Cancer Cell* **19,** 192–205
29. Wei, W., Zeve, D., Wang, X., Du, Y., Tang, W., Dechow, P. C., Graff, J. M., and Wan, Y. (2011) Osteoclast progenitors reside in the peroxisome proliferator-activated receptor $\gamma$-expressing bone marrow cell population. *Mol. Cell Biol.* **31,** 4692–4705
30. Rodda, S. J., and McMahon, A. P. (2006) Distinct roles for Hedgehog and canonical Wnt signaling in specification, differentiation and maintenance of osteoblast progenitors. *Development* **133,** 3231–3244
31. Furth, P. A., St Onge, L., Böger, H., Gruss, P., Gossen, M., Kistner, A., Bujard, H., and Hennighausen, L. (1994) Temporal control of gene expression in transgenic mice by a tetracycline-responsive promoter. *Proc. Natl. Acad. Sci. U.S.A.* **91,** 9302–9306
32. Kalajzic, I., Kalajzic, Z., Kaliterna, M., Gronowicz, G., Clark, S. H., Lichtler, A. C., and Rowe, D. (2002) Use of type I collagen green fluorescent protein transgenes to identify subpopulations of cells at different stages of the osteoblast lineage. *J. Bone Miner. Res.* **17,** 15–25
33. Irwin, N. (1989) in *Molecular Cloning: A Laboratory Manual* (Sambrook, J., Fritsch, E. F., and Maniatis, T., eds) Cold Spring Harbor Laboratory Press, Cold Spring Harbor, NY
34. Garnero, P., Borel, O., and Delmas, P. D. (2001) Evaluation of a fully automated serum assay for C-terminal cross-linking telopeptide of type I collagen in osteoporosis. *Clin. Chem.* **47,** 694–702
35. Bouxsein, M. L., Boyd, S. K., Christiansen, B. A., Guldberg, R. E., Jepsen, K. J., and Müller, R. (2010) Guidelines for assessment of bone microstructure in rodents using micro-computed tomography. *J. Bone Miner Res.* **25,** 1468–1486
36. Gazzerro, E., Pereira, R. C., Jorgetti, V., Olson, S., Economides, A. N., and Canalis, E. (2005) Skeletal overexpression of gremlin impairs bone formation and causes osteopenia. *Endocrinology* **146,** 655–665
37. Parfitt, A. M., Drezner, M. K., Glorieux, F. H., Kanis, J. A., Malluche, H., Meunier, P. J., Ott, S. M., and Recker, R. R. (1987) Bone histomorphometry: standardization of nomenclature, symbols, and units. Report of the ASBMR Histomorphometry Nomenclature Committee. *J. Bone Miner. Res.* **2,** 595–610
38. McCarthy, T. L., Centrella, M., and Canalis, E. (1990) Cyclic AMP induces insulin-like growth factor I synthesis in osteoblast-enriched cultures. *J. Biol. Chem.* **265,** 15353–15356
39. Akazawa, C., Sasai, Y., Nakanishi, S., and Kageyama, R. (1992) Molecular characterization of a rat negative regulator with a basic helix-loop-helix structure predominantly expressed in the developing nervous system. *J. Biol. Chem.* **267,** 21879–21885
40. Lian, J., Stewart, C., Puchacz, E., Mackowiak, S., Shalhoub, V., Collart, D., Zambetti, G., and Stein, G. (1989) Structure of the rat osteocalcin gene and regulation of vitamin D-dependent expression. *Proc. Natl. Acad. Sci. U.S.A.* **86,** 1143–1147
41. Iso, T., Sartorelli, V., Poizat, C., Iezzi, S., Wu, H. Y., Chung, G., Kedes, L., and Hamamori, Y. (2001) HERP, a novel heterodimer partner of HES/E(spl) in Notch signaling. *Mol. Cell Biol.* **21,** 6080–6089
42. Kouadjo, K. E., Nishida, Y., Cadrin-Girard, J. F., Yoshioka, M., and St-Amand, J. (2007) Housekeeping and tissue-specific genes in mouse tissues. *BMC. Genomics* **8,** 127
43. Tso, J. Y., Sun, X. H., Kao, T. H., Reece, K. S., and Wu, R. (1985) Isolation and characterization of rat and human glyceraldehyde-3-phosphate dehydrogenase cDNAs: genomic complexity and molecular evolution of the gene. *Nucleic Acids Res.* **13,** 2485–2502
44. Takahashi, N., Akatsu, T., Udagawa, N., Sasaki, T., Yamaguchi, A., Moseley, J. M., Martin, T. J., and Suda, T. (1988) Osteoblastic cells are involved in osteoclast formation. *Endocrinology* **123,** 2600–2602
45. Lee, S. K., Kalinowski, J., Jastrzebski, S., and Lorenzo, J. A. (2002) 1,25(OH)2 vitamin D3-stimulated osteoclast formation in spleen-osteoblast cocultures is mediated in part by enhanced IL-1$\alpha$ and receptor activator of NF-$\kappa$B ligand production in osteoblasts. *J. Immunol.* **169,** 2374–2380
46. Wyzga, N., Varghese, S., Wikel, S., Canalis, E., and Sylvester, F. A. (2004) Effects of activated T cells on osteoclastogenesis depend on how they are activated. *Bone* **35,** 614–620

47. Sokal, R. R., and Rohlf, F. J. (1981) *Biometry*, 2nd Edition, W. H. Freeman, San Francisco, CA
48. Canalis, E., Parker, K., Feng, J. Q., and Zanotti, S. (2013) Osteoblast lineage-specific effects of notch activation in the skeleton. *Endocrinology* **154,** 623–634
49. Hildebrand, T., and Rüegsegger, P. (1997) Quantification of bone microarchitecture with the Structure Model Index. *Comput. Methods Biomech. Biomed. Engin.* **1,** 15–23
50. Mundy, G. R. (2007) Osteoporosis and inflammation. *Nutr. Rev.* **65,** S147–S151
51. Boban, I., Jacquin, C., Prior, K., Barisic-Dujmovic, T., Maye, P., Clark, S. H., and Aguila, H. L. (2006) The 3.6 kb DNA fragment from the rat Col1a1 gene promoter drives the expression of genes in both osteoblast and osteoclast lineage cells. *Bone* **39,** 1302–1312
52. Scheller, E. L., Leinninger, G. M., Hankenson, K. D., Myers, M. G., Jr., and Krebsbach, P. H. (2011) Ectopic expression of Col2.3 and Col3.6 promoters in the brain and association with leptin signaling. *Cells Tissues Organs* **194,** 268–273
53. Manolagas, S. C., Kousteni, S., and Jilka, R. L. (2002) Sex steroids and bone. *Recent Prog. Horm. Res* **57,** 385–409
54. O'Brien, C. A., Lin, S. C., Bellido, T., and Manolagas, S. C. (2000) Expression levels of gp130 in bone marrow stromal cells determine the magnitude of osteoclastogenic signals generated by IL-6-type cytokines. *J. Cell Biochem.* **79,** 532–541
55. Yoshitake, F., Itoh, S., Narita, H., Ishihara, K., and Ebisu, S. (2008) Interleukin-6 directly inhibits osteoclast differentiation by suppressing receptor activator of NF-$\kappa$B signaling pathways. *J. Biol. Chem.* **283,** 11535–11540